

UNCLASSIFIED

N00014-81-K-0664

NL

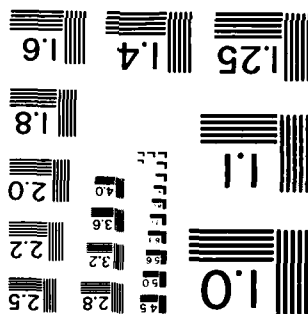
F/G 11/6

END

FILMED

DTAC

MICROCOPY RESOLUTION TEST CHART
NATIONAL BUREAU OF STANDARDS - 1963-A



AD-A148 240

DTIC FILE COPY

SECURITY CLASSIFICATION OF THIS PAGE (When Data Entered)

REPORT DOCUMENTATION PAGE		READ INSTRUCTIONS BEFORE COMPLETING FORM
1. REPORT NUMBER Technical Report No. 4	2. GOVT ACCESSION NO.	3. RECIPIENT'S CATALOG NUMBER
4. TITLE (and Subtitle) Fluctuation Phenomena Studies in Chemically Sensitive Field Effect Transistor Part I. Corrosion of Aluminum		5. TYPE OF REPORT & PERIOD COVERED Interim Technical Report
6. AUTHOR(s) Zheng Kang Li, J. M. Reijn and J. Janata		7. PERFORMING ORG. REPORT NUMBER
8. CONTRACT OR GRANT NUMBER(s) N00014-81-K-0664		9. PROGRAM ELEMENT, PROJECT, TASK AREA & WORK UNIT NUMBERS NR 051-77815-79-81(472)
10. PERFORMING ORGANIZATION NAME AND ADDRESS Department of Bioengineering University of Utah Salt Lake City, Utah 84112		11. REPORT DATE November 20, 1984
12. CONTROLLING OFFICE NAME AND ADDRESS G. Max Irving, Office of Naval Research University of New Mexico, Room 204, Bandolier Hall West, Albuquerque, New Mexico 87131		13. NUMBER OF PAGES
14. MONITORING AGENCY NAME & ADDRESS (if different from Controlling Office)		15. SECURITY CLASS. (of this report)
		16. DECLASSIFICATION/DOWNGRADING SCHEDULE
17. DISTRIBUTION STATEMENT (of this Report) Approved for public release: distribution unlimited		
18. DISTRIBUTION STATEMENT (of the abstract entered in Block 20, if different from Report)		
19. SUPPLEMENTARY NOTES Accepted for publication in J. Electrochem. Soc.		
20. KEY WORDS (Continue on reverse side if necessary and identify by block number) Chemically Sensitive Field Effect Transistor; Fluctuation Analysis; Corrosion of Aluminum		
21. ABSTRACT (Continue on reverse side if necessary and identify by block number) It is shown that chemically sensitive field effect transistors can be used to study stochastic processes at the solution/solid interface which is not at equilibrium. Auto spectral densities and coherence functions for corrosion of aluminum-silicon alloy at zero-net current conditions have been obtained.		

DTIC
SELECTED
DEC 5 1984
D

Accession For	
NTIS GRA&I	X
DTIC TAB	
Unannounced	
Justification	
By	
Distribution/	
Availability Codes	
Dist	Avail and/or Special
A/1	

FLUCTUATION PHENOMENA STUDIES IN CHEMICALLY

SENSITIVE FIELD EFFECT TRANSISTORS

PART I. CORROSION OF ALUMINUM

Zheng Kang Li, Johannes M. Reijn and Jiří Janata
 University of Utah
 Department of Bioengineering
 Salt Lake City, Utah 84112

Submitted to J. Electrochem. Soc.
 Descriptors: Alloy, Etching, Integrated Circuits, Surfaces

DTIC
 ELECTE
 DEC 5 1984
 S D

DISSEMINATION STATEMENT A
 Approved for public release
 Distribution Unlimited

ABSTRACT

It is shown that chemically sensitive field effect transistors can be used to study stochastic processes at the solution/solid interface which is not at equilibrium. Auto spectral densities and coherence functions for corrosion of aluminum-silicon alloy at zero-net current conditions have been obtained.

INTRODUCTION

Noise in chemically sensitive field effect transistors (CHEMFET) originates both from the solid state part of the device and from the electrochemical processes at each interface. In our previous work we have shown that the analysis of noise of CHEMFETs with various ion selective membranes at chemical equilibrium yields an information about the exchange currents at the solution/membrane interface and about the bulk impedance of the membrane itself [1].

High signal-to-noise ratio, small input capacitance, small surface area of the electrode and low parasitic impedance are the attractive features of CHEMFETs for the study of stochastic processes in electrochemical systems. Because each chip contains at least two transistors, it is possible to use multichannel analysis methods. These methods can yield an unique additional information about the whole system and they reduce contributions from the solid state part of the system.

In the first part of this series, we shall outline the theory of noise analysis in CHEMFETs and describe the experimental arrangement which was used in this and the subsequent studies.

PRINCIPLE OF OPERATION

The basic operation of CHEMFETs has been described elsewhere [2]. The output, drain-to-source current I_D , for a n-channel transistor operated in the non-saturated region $[V_D < (V_G - V_T)]$ is:

$$I_D = K \left[(V_G - V_T) - \frac{V_D}{2} \right] V_D \quad (1)$$

and in the saturation region where $V_D > (V_G - V_T)$:

$$I_D = K' (V_G - V_T)^2 \quad (2)$$

The constants K and K' are characteristic of the geometry and material properties of the transistor shown in Fig. 1. The transconductance of the transistor is defined as

$$g_m = \left(\frac{\partial I_D}{\partial V_G} \right)_{V_D} \quad (3)$$

Because the magnitude of the solid state part of the noise depends on the value of the drain current, it is preferable to operate the transistor in so called feedback mode in which the average drain current is kept constant. In this case, the gate voltage fluctuations $v(t)$ are transformed into the drain

current fluctuations $i(t)$ through the relationship:

$$i(t) = g_m v(t) \quad (4)$$

FLUCTUATION ANALYSIS THEORY

In this section a brief review of theory relevant to the present experiments is given. For a fuller account of the theoretical background the reader is referred to textbooks [3-5]. The drain current in the channel $I_D(t)$ of an ISFET can be expressed as [1]:

$$I_D(t) = \bar{I} + i(t) \quad (5)$$

Where \bar{I} is the mean value of the current and $i(t)$ is the fluctuating part of the drain current (noise). In the remaining part of this text we will consider the fluctuations in the drain current only and for the sake of notation describe drain current fluctuations as $x(t)$ or $y(t)$.

When one is interested in the origin of the fluctuations, characterization of the signal (by means of parameters for instance) is necessary. Before any meaningful signal characterization can be attempted, the signal has to be qualified.

This qualification can be carried out in the following way: Figure 2 shows graphically the concept of a Probability Density Function (PDF) which is defined for the signal $x(t)$ as:

$$p(x) = \lim_{\Delta x \rightarrow 0} \frac{\text{Prob}[x < x(t) < x + \Delta x]}{\Delta x}$$

In general $p(x,t)$ is a function of time. If this is not the case, that is when $p(x,t_1) = p(x,t_2)$ for all t_1, t_2 , it is said that the fluctuating signal is stationary. By its definition the PDF $p(x,t)$ is normalized, i.e.,

$\int p(x,t)dx = 1$, where the integration is carried out over all values of the signal $x(t)$. For the PDF statistical moments can be calculated in the usual way, e.g., [6]. A large class of signals is formed by signals with a Gaussian PDF as illustrated in Fig. 2. When a fluctuating signal of this class has 'direct' statistical moments defined by:

-mean value:

$$\langle x(t) \rangle = \lim_{T \rightarrow \infty} \left(\frac{1}{T} \int_0^T x(t) dt \right) \quad (6)$$

-mean value of the square:

$$\langle x^2(t) \rangle = \lim_{T \rightarrow \infty} \left(\frac{1}{T} \int_0^T x^2(t) dt \right) \quad (7)$$

-variance:

$$\sigma_t^2 = \langle x^2(t) \rangle - \langle x(t) \rangle^2 \quad (8)$$

When the measuring time is taken long enough (usually a limit $T \rightarrow \infty$ is involved) and the above defined moments equal the corresponding moments of the PDF for a stationary fluctuation, the signal is ergodic.

FREQUENCY DOMAIN ANALYSIS

When the signal is stationary and ergodic its parameters are independent of the observation time. This property allows for analysis of signal parameters from individual time records, e.g., mean and variance or from many different records as e.g. for frequency analysis using sampled portions of the signal of finite length (to be referred to as ensembles).

Suppose that one ensemble is represented by N samples, taken at time intervals Δt ; N is usually an integer power of 2. From the sequence of samples one calculates a Discrete Fourier Transform (DFT), usually using a Fast Fourier Transform algorithm (FFT) to save computation time [7]. From the Fourier components estimates of spectral densities $G_x(k)$ are calculated as discrete frequencies $k f_0$, unique up to $k = N/2 - 1$. The sequence $G_x(k)$ is a discrete representation of the auto spectral density function for the signal $X(t)$. The true, continuous, single-continuous, single-sided auto spectral density $G_x(f)$ is defined as:

$$G_x(f) = 2 \lim_{T \rightarrow \infty} \frac{1}{T} \int_0^T X_k(f, T)^2 dT \quad (9)$$

The random part of the error in the spectral estimates is given by Bendat and Piersol [3] for the case of a signal with a Gaussian PDF as a normalized standard error:

$$\epsilon_T = \sqrt{2/M} \quad (10)$$

where M equals the number of degrees of freedom in statistical sense (each time record has two degrees of freedom due to the fact that the spectral estimate has a real and an imaginary component). This implies that the standard deviation in a spectral estimate calculated from one time record is 100%, independent of the length of the record.

The number of degrees of freedom can be increased in two ways: by smoothing of the estimates at the expense of spectral resolution or by segment averaging. The latter technique requires a longer observation time, but preserves the spectral resolution, and is, therefore, adopted in this paper.

The bias part of the error in the spectral estimates is a function of the 'shape' of the spectral density function. For flat spectra, 1/f noise and Lorentzian spectra this error is negligibly small at the frequencies of interest [3].

From the definition of the spectral density it follows immediately that if a signal can be considered to be the sum of some stationary, ergodic signals the spectral density of the sum equals the sum of the spectral densities of the individual signals:

$$\begin{aligned} x(t) &= \sum_i x_i(t) & i &= 1, 2, 3 \dots \\ G_x(f) &= \sum_i G_{x_i}(f) & i &= 1, 2, 3 \dots \end{aligned} \quad (11)$$

In a previous paper [1] this property was used by Haemmerli et al. to discriminate between noise originating in different parts of the ISFET/electrochemical cell system. It is clear from eq. (11) that as soon as

one of the different noise sources is stronger than the others this discrimination becomes impossible. The same conclusion was reached by Haemmerli.

TWO CHANNEL APPROACH

In order to reduce the device noise in a ISFET/electrochemical system, a two channel approach was developed based on the following reasoning: Suppose that two ISFETs have an electrochemical noise source in common but that their 'solid state' noise is not correlated. For the fluctuations in the two drain currents we can write:

$$\begin{aligned} x(t) &= d_1(t) + e(t) \\ y(t) &= d_2(t) + e(t) \end{aligned} \quad (12)$$

$d_1(t)$ is the device noise for FET1, $d_2(t)$ is the device noise for FET2 and $e(t)$ is the (electrochemical) noise common to both channels. The true continuous single-side spectral density functions are:

$$\begin{aligned} G_x(f) &= [D_1(f) + E(f)][D_1(f) + E(f)]^* \\ G_y(f) &= [D_2(f) + E(f)][D_2(f) + E(f)]^* \\ G_{xy}(f) &= [D_2(f) + E(f)][D_1(f) + E(f)]^* \end{aligned} \quad (13)$$

where (*) denotes a complex conjugate. $D_1(f)$ and $D_2(f)$ are Fourier transforms of signals $d_1(t)$ and $d_2(t)$, $E(f)$ is the Fourier transform of the noise $e(t)$ common to both channels. If we drop the frequency dependence for convenience of notation, expanded eq. (13) becomes:

$$\begin{aligned} G_x &= D_1 D_1^* + E D_1^* + D_1 E^* + E E^* \\ G_y &= D_2 D_2^* + E D_2^* + D_2 E^* + E E^* \\ G_{xy} &= D_2 D_1^* + D_2 E^* + E D_1^* + E E^* \end{aligned} \quad (14)$$

If d_1 , d_2 and e are uncorrelated noise sources all cross-terms in eq. (14):

$$E D_1^* = D_1 E^* = E D_2^* = D_2 E^* = D_1 D_2^* = D_2 D_1^*$$

are zero and hence:

$$\begin{aligned} G_x &= D_1 D_1^* + E E^* \\ G_y &= D_2 D_2^* + E E^* \\ G_{xy} &= E E^* \end{aligned} \quad (15)$$

The cross spectral density function is thus a function of electrochemical noise common to both channels only.

A derived quantity is the coherence function defined as:

$$\gamma(f)^2 = \frac{|G_{xy}(f)|^2}{G_x(f) G_y(f)} \quad (16)$$

Theoretically, this function has a range from zero for no coherence to one for complete coherence. It can be viewed as a measure for the amount of signal common to both channels.

The same considerations as above apply to the statistical errors in estimates of the auto spectral density functions obtained by Fourier analysis of time records. Error estimates in the cross power spectral density and in the coherence function are dependent on the amount of coherence between the two signals and are relatively complicated [3,8]. The number of degrees of freedom is important especially at low levels of coherence as Table 1 shows:

TABLE 1

Error estimate in coherence function at 99% confidence
level and for coherence = 0.01

<u>Degrees of Freedom</u>	<u>Lower Limit</u>	<u>Upper Limit</u>
100	0	.06
1000	.002	.022
10000	.007	.013

EXPERIMENTAL

The transistor chips used in this study are identical to those used previously [1]. They were mounted on 1.5 mm diameter PVC tubing and encapsulated with a high-grade epoxy resin (Epon 826 with Jeffamine D230 crosslinker). The two gates used for the cross-correlation measurements are connected as shown in Fig. 1. In this study we have used 25 μm diameter Al-Si (1%) wire, the geometrical area of the metal exposed to the solution was approximately $7 \times 10^{-6} \text{ cm}^2$. During etching experiments this area was renewed by cutting the sample perpendicularly to the wire axis after each experiment. Unless stated otherwise, the measurements were done at room temperature. The actual temperature at the sensor site was determined by pre-calibration of one of the MOSFETS available on the transistor chip.

The noise measurements were done under two sets of experimental conditions: in pH 9.0, 0.1 M borate buffer (no corrosion) and in etching solution consisting of 1600 ml H_3PO_4 (35% Fisher) 100 ml HNO_3 (69% Fisher), 100 ml acetic acid (glacial, Fisher) and 200 ml of water. This solution was diluted with distilled deionized water for concentration dependence studies as necessary. The solutions were degassed with nitrogen and stored in glass bottles under nitrogen. They were delivered to the transistor under constant pressure using the manifold shown in Fig. 3. The volumetric flow rate was controlled by adjusting the nitrogen pressure. Because of the irregular geometry of the encapsulated sample, the absolute face velocity of the flowing solution at the sample surface could not be determined. The electrical circuits used for monitoring the drain-to-source current are shown for a two-channel operation in Fig. 4.b. The output signals were amplified with low noise, variable gain (1-10 K) pre-amplifiers (Princeton Applied Research, Model PARC113A) and analyzed using Hewlett-Packard Signal Analyzer (HP 3582A).

The accessible frequencies of this measuring setup were between 0.8 Hz and 25 kHz.

RESULTS

In the preliminary experiments we have used diluted hydrochloric acid (0.1 mM to 0.1M) as the reaction medium. For concentrations above 5mM HCl the reaction was too violent yielding bubbles of hydrogen which created problems in the flow cell. For concentrations below 1 mM the change of surface pH due to low buffering capacity led to irreproducible results. Nevertheless, the auto spectral densities in these experiments exhibited a pronounced maximum in the region between 1-10 Hz which increased with increasing concentration of the acid from $5 \times 10^{-18} \text{ A}^2 \text{ Hz}^{-1}$ for 0.1 mM HCl to $5 \times 10^{-17} \text{ A}^2 \text{ Hz}^{-1}$ for 0.1 M HCl

In order to control the surface concentrations better a buffered solution normally used for etching aluminum in the integrated circuit fabrication process [9] has been used in various dilutions. For undiluted solutions at room temperature the typical etching rate is less than $1000 \text{ \AA min}^{-1}$. Therefore, for the duration of our experiment (~10 min.) the removal of the material has not significantly altered the flow pattern around the sample.

The auto spectral densities for etching solutions of various dilutions are shown in Fig. 5. These are the results of 128 averages. There is a clear evidence of a Lorentzian character of the spectrum (slope -2) for the two highest concentrations. The intensity of the spectrum increases with the increasing concentration of the etching solution in general agreement with the results obtained with hydrochloric acid.

The coherence function (eq. 16) for the data presented in Fig. 5 is shown in Fig. 6. It again shows the expected concentration dependence. In

buffer solution where no significant corrosion takes place, its value is 0.025 and independent of frequency up to 1 kHz. The fact that the coherence has a non-zero value indicates the presence of common electrochemical noise which probably originates from the pseudo-exchange current (non-equilibrium) which takes place at the metal/solution interface. This statement has to be taken within the context of the statistical accuracy of the coherence function (Table 1).

CONCLUSION

In this paper we have outlined the framework for study of non-equilibrium fluctuation phenomena in chemically sensitive field effect transistors both from the theoretical and from the experimental point of view. The corrosion of aluminum/silicon alloy is used only as an illustration that this approach is feasible and no interpretation of the experiments is attempted. The corrosion of metals and semiconductors is commonly studied by conventional electrochemical means in which the important corrosion parameters are derived from current-voltage characteristics which are extrapolated to zero net current conditions. Bertocci [10-12] has introduced the concept of coherence to corrosion measurements. It has allowed him to determine the causal relationship between current and voltage. The fundamental difference in our measurements is that they are performed at zero-net current condition. Thus, the only independent variables are surface concentrations, temperature and pressure. This approach is possible because the coupling between the electrochemical process and the interface and the observable (fluctuation of the drain-to-source current) is through the electric field. In the following paper we will show that this mode of operation yields an unique approach to the study of electrochemical reactions of various materials, including insulators.

ACKNOWLEDGEMENTS

This work was supported by the contract from the Office of Naval Research. We are indebted to our colleagues, Professors J. J. Brophy and Martin Fleischmann for stimulating discussions and encouragement.

Figure 1. Schematic diagram of the transistor chip (drawing not to scale).

D - drain, S - source, I - insulator, M - metal, E - encapsulant, R - reference electrode, and SB - substrate. I_D is drain-to-source current and V_G is the applied gate voltage

Figure 2. Illustration of Probability Density Function (PDF) for an arbitrary signal. (a) Time record, (b) PDF.

Figure 3. Experimental arrangement. A, the amplifier, P, battery pack, T, the transistor under study, REF, the reference electrode, F, the flow-cell, H, the heater, S, the solution inlet, W, the outlet to waste, O, the amplifier output, V's are control valves, L, the hydrodynamic load, E, the etching solution, and B, the buffer (---), Faraday shielding.

Figure 4. Circuit used in two-channel measurements; REF - reference electrode; E_{OUT} - output voltage; D - drain; S - source.

Figure 5. Autospectral density for corrosion of aluminum at three different concentrations of etching solution. Vertical axis current density units are in A^2/Hz .

Figure 6. Coherence function obtained in two channel mode for three different concentrations of etching solution and for buffer solution.

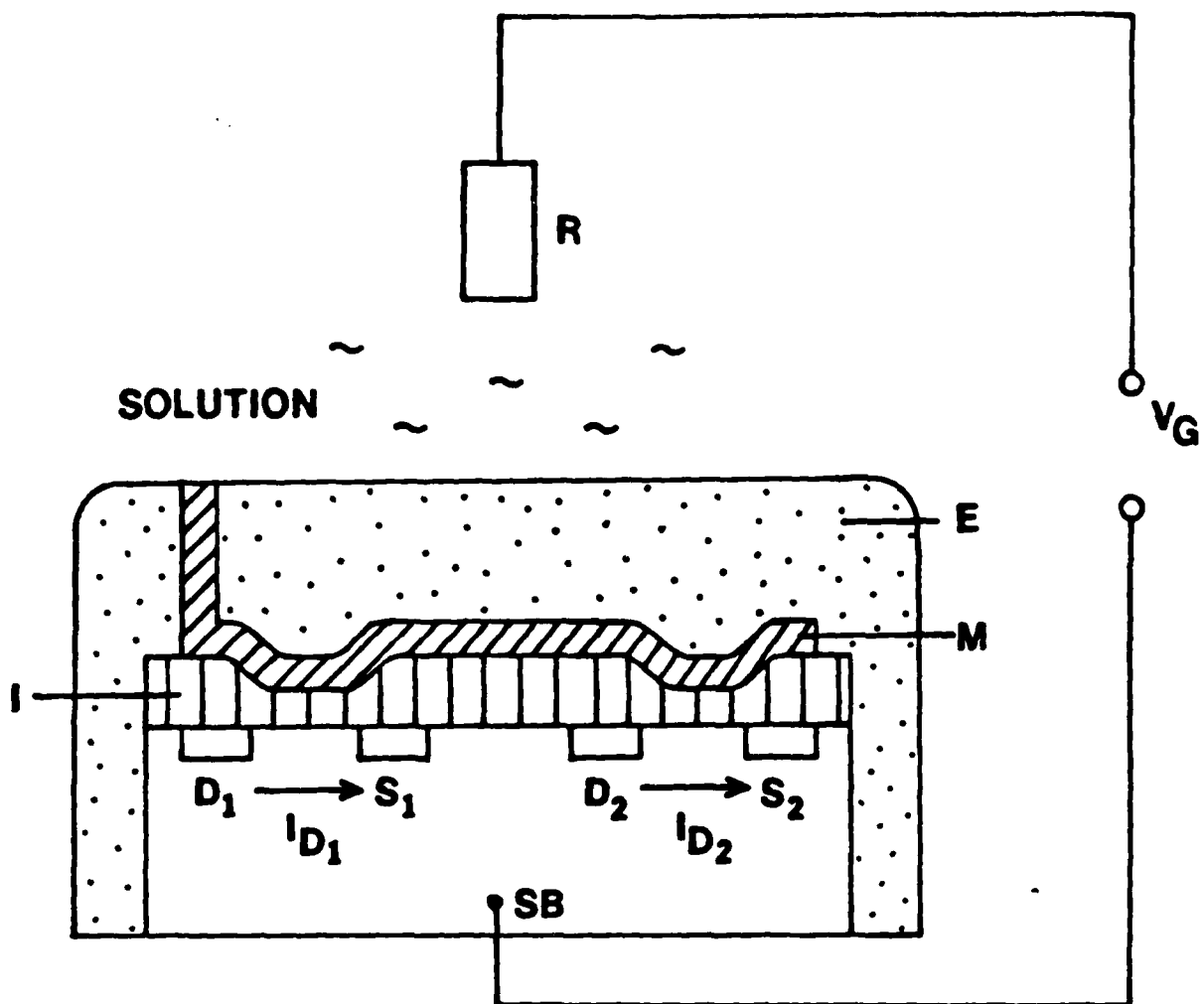


Fig. 1

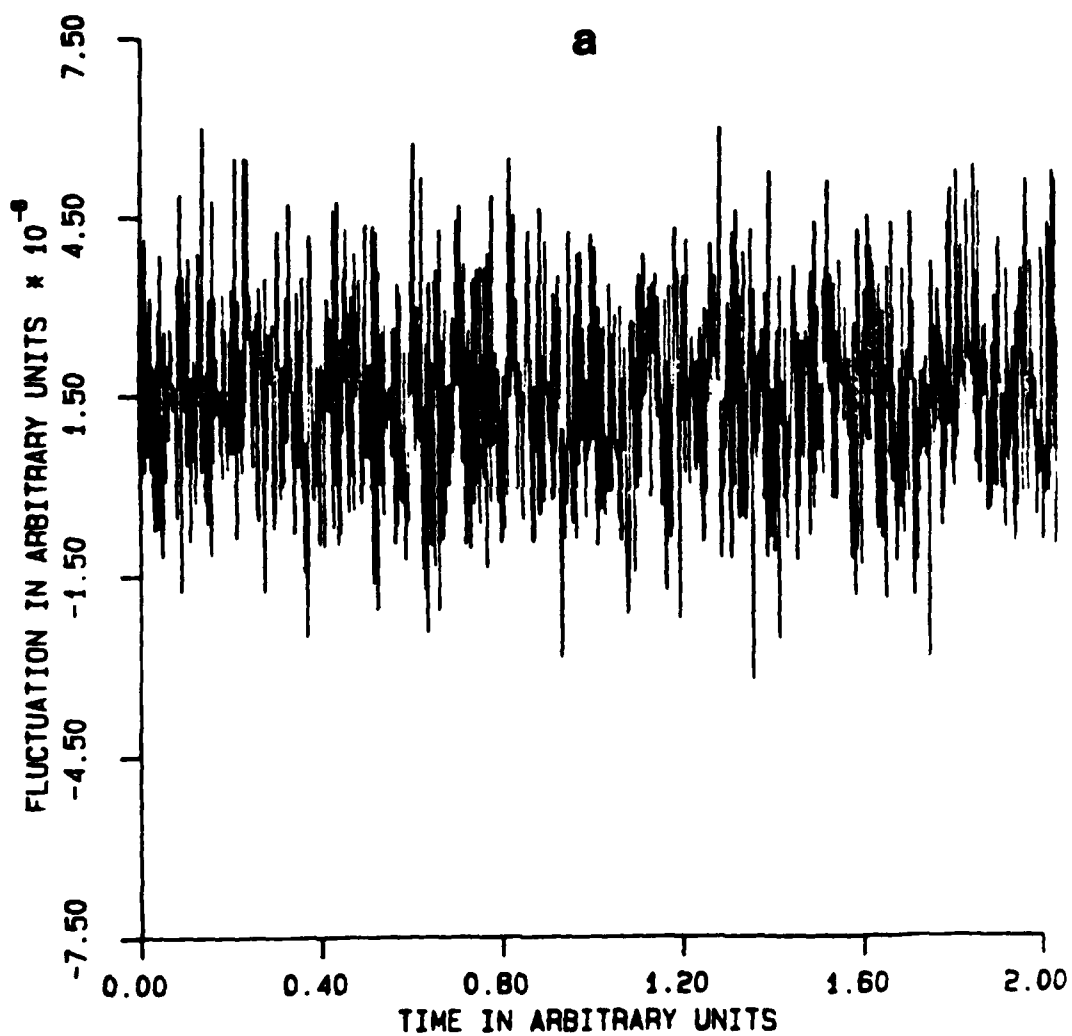


Fig. 2a

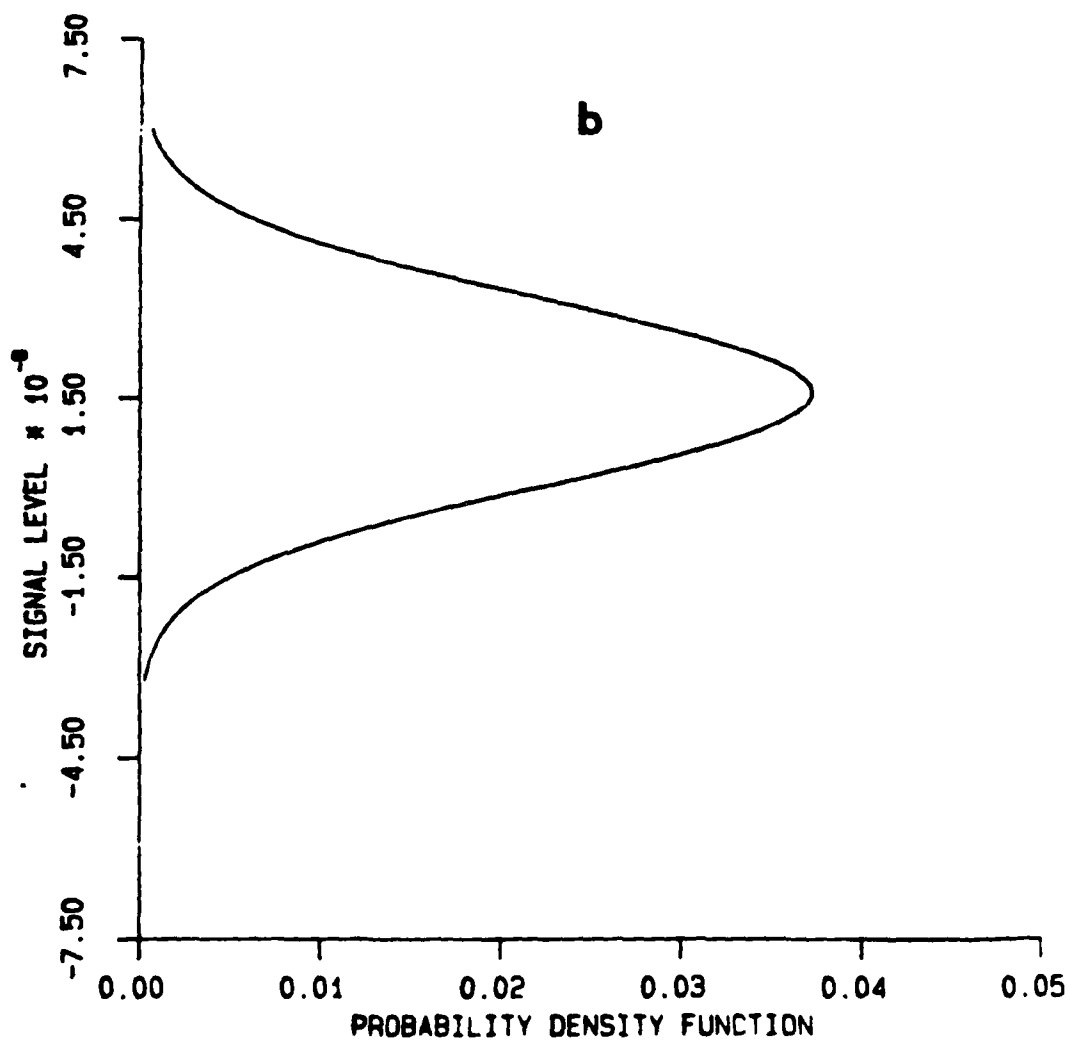


Fig. 26

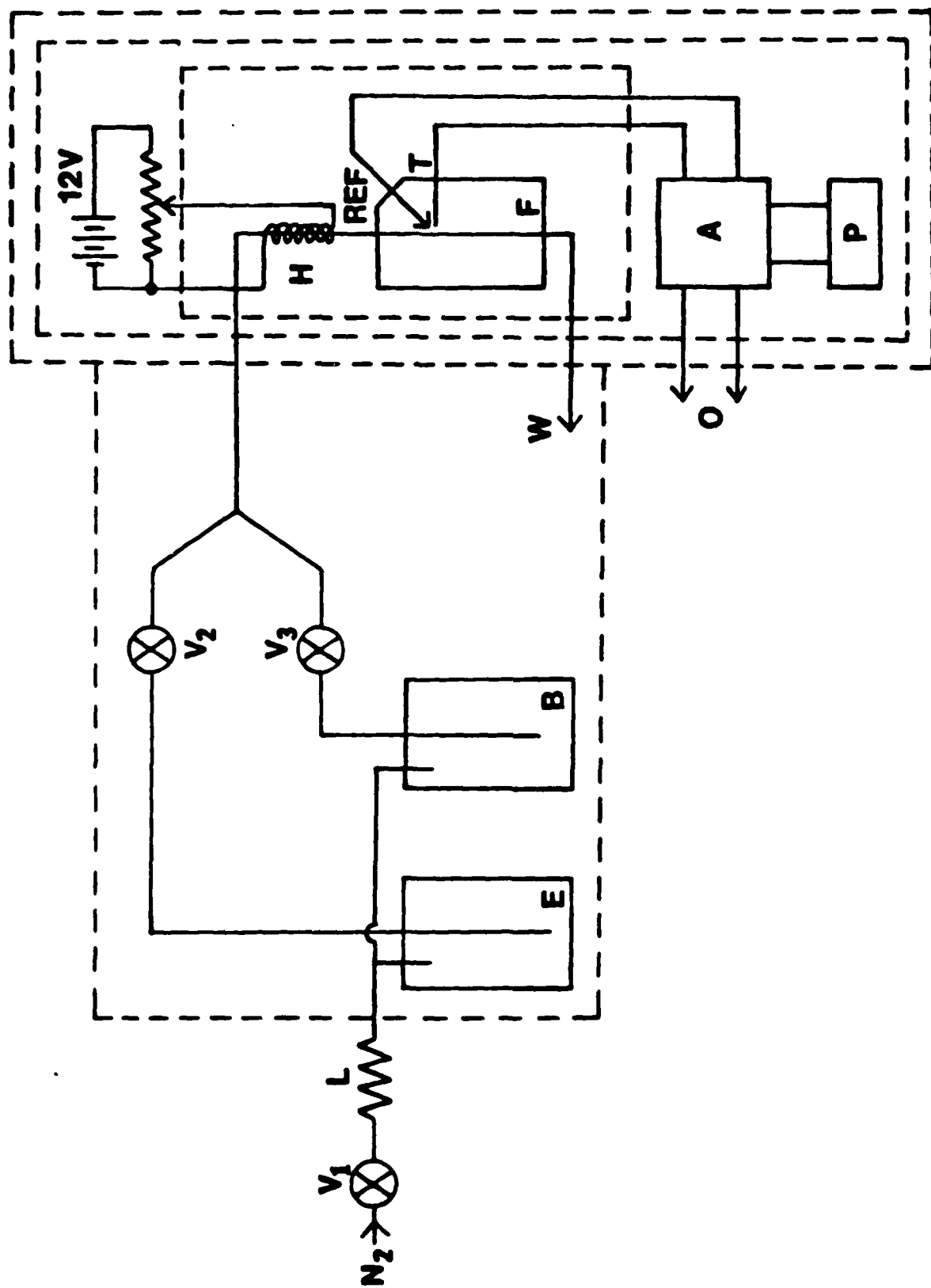


Fig. 3

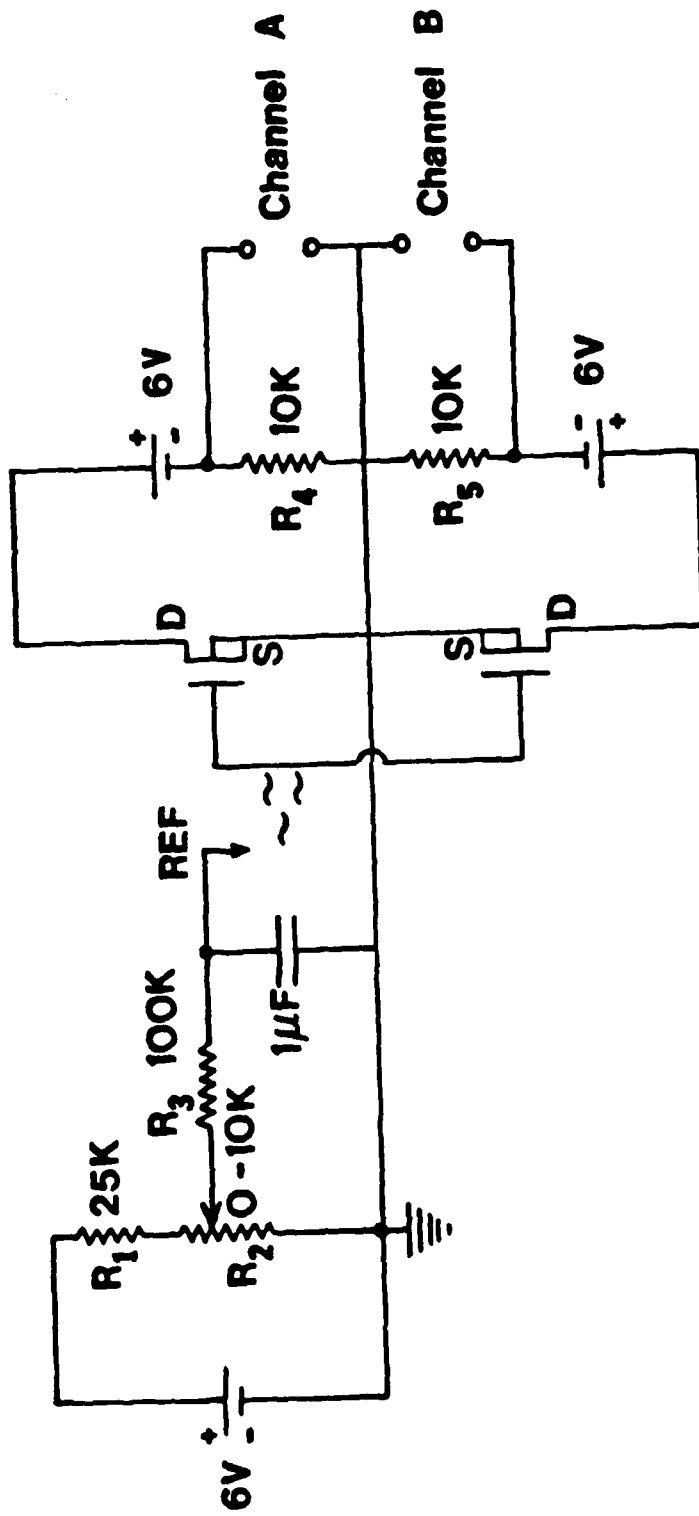


Fig. 4b

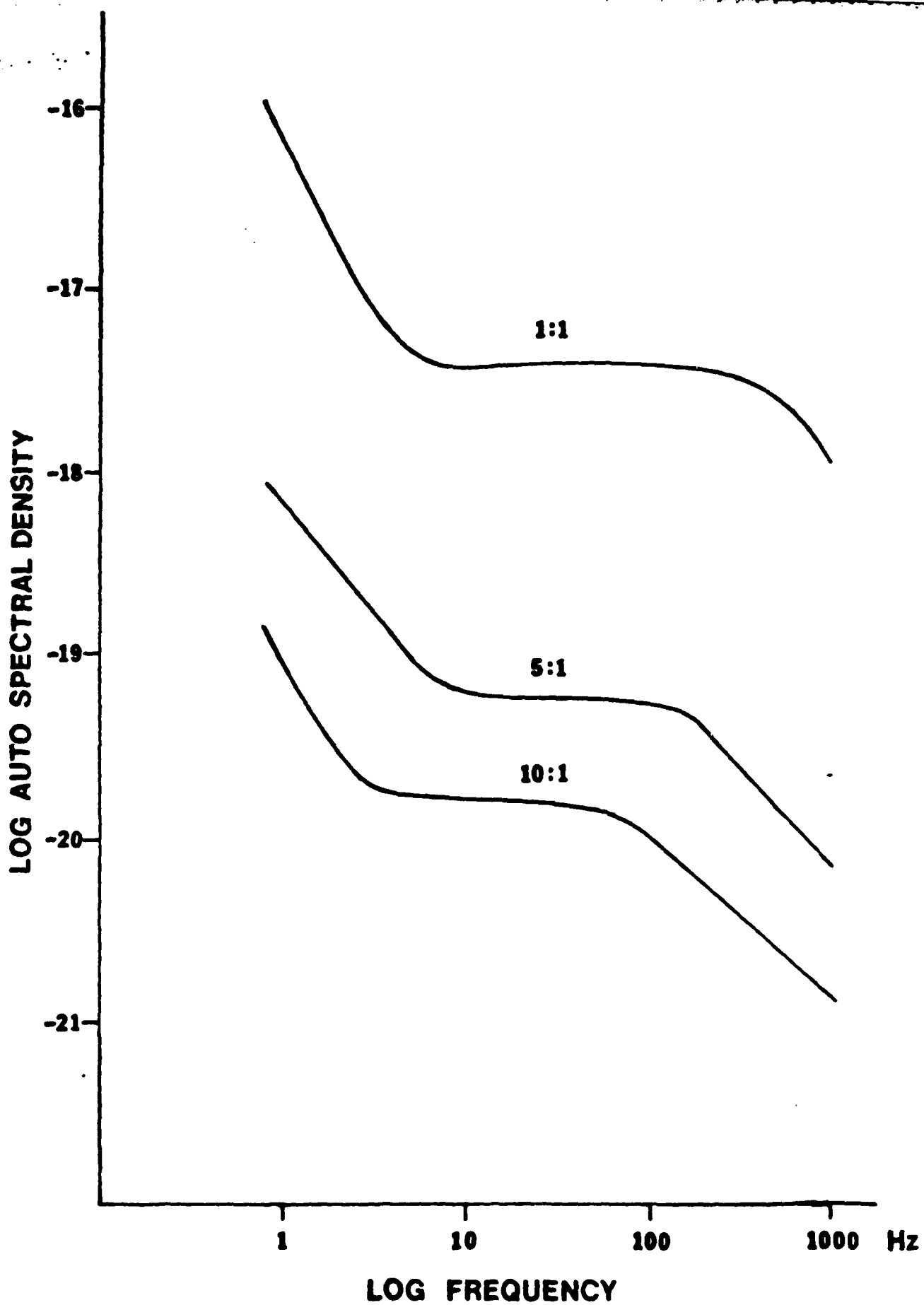


Fig. 5

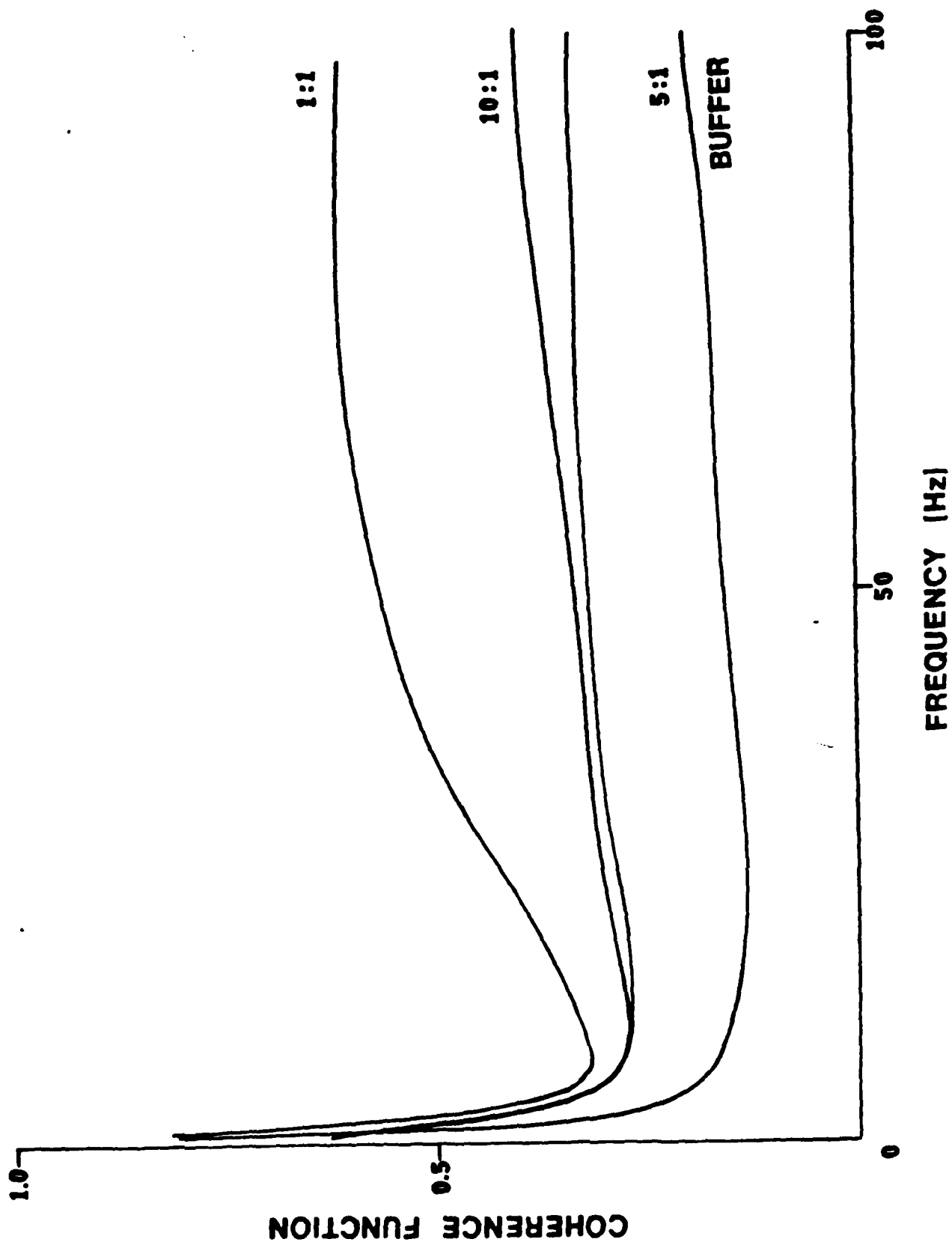


Fig. 6

LIST OF SYMBOLS

$D(f)$	Fourier transform of device noise
$E(f)$	Fourier transform of electrochemical noise
$d(t)$	Device noise in time domain
$e(t)$	Electrochemical noise in time domain
V_D	Drain-source voltage
V_G	Gate-source voltage
V_T	Threshold voltage
I_D	Drain current
\bar{I}_D	Average value of drain current
$i(t)$	Fluctuation in drain current in time domain
g_m	Transconductance of FET
K, K'	Constants of FET
$v(t)$	Fluctuations in gate voltage
$x(t)$	Fluctuating signal in time domain
$y(t)$	Fluctuating signal in time domain
$p(x, t)$	Probability density function for $x(t)$
$\langle x \rangle$	Mean value of signal $x(t)$
$\langle x^2 \rangle$	Mean value of the square for $x(t)$
σ_t	Variance of $x(t)$
$G_x(f)$	Auto spectral density for signal $x(t)$
$G_y(f)$	Auto spectral density for signal $y(t)$
$G_{xy}(f)$	Cross spectral density for signals $x(t)$ and $y(t)$
N	Number of samples in finite length discrete time record
M	Number of averages in spectral density estimate
$\gamma^2(f)$	Coherence function

REFERENCES

1. A. Haemmerli, J. Janata and J.J. Brophy, This Journal, 129, 2307(1982).
2. J. Janata and R.J. Huber in, "Ion Selective Electrodes in Analytical Chemistry," Vol. 2, H. Freiser ed., Plenum Press, New York (1980).
3. J.S. Bendat and A.G. Piersol, "Random Data: Analysis and Measurement Procedures," Wiley-Interscience, New York (1971).
4. R.N. Bracewell,, "The Fourier Transform and its Applications," Second Edition McGraw-Hill, New York (1978).
5. C.W. Gardiner, "Handbook of Stochastic Methods for Physics, Chemistry and the Natural Sciences," Springer Verlag, Berlin (1983).
6. M. Abramowitz, I.A. Stegun, "Handbook of Mathematical Functions," Chap. 26, Dover, New York (1963).
7. J.W. Cooley, J.W. Tukey, Math. Comp. 19, 297(1965).
8. V.A. Benignus, IEEE Trans. Audio Electroacoustics, Vol. AU-17, 145(1969).
9. D.J. Elliott, "Integrated Circuit Fabrication Technology," Chap. 11, McGraw-Hill, New York (1982).
10. U. Bertocci, This Journal, 127, 1931(1980).
11. U. Bertocci, This Journal 128, 520 (1981).
12. U. Bertocci in, "Proceedings of the Sixth International Conference on Noise in Physical Systems," p. 328 National Bureau of Standards, Washington (1981).

TECHNICAL REPORT DISTRIBUTION LIST, GEN

	<u>No. Copies</u>		<u>No. Copies</u>
Office of Naval Research Attn: Code 413 800 N. Quincy Street Arlington, Virginia 22217	2	Dr. David Young Code 334 NORDA NSTL, Mississippi 39529	1
Dr. Bernard Doua Naval Weapons Support Center Code 5042 Crane, Indiana 47522	1	Naval Weapons Center Attn: Dr. A. B. Amster Chemistry Division China Lake, California 93555	1
Commander, Naval Air Systems Command Attn: Code 310C (H. Rosenwasser) Washington, D.C. 20360	1	Scientific Advisor Commandant of the Marine Corps Code RD-1 Washington, D.C. 20380	1
Naval Civil Engineering Laboratory Attn: Dr. R. W. Drisko Port Hueneme, California 93401	1	U.S. Army Research Office Attn: CRD-AA-IP P.O. Box 12211 Research Triangle Park, NC 27709	1
Defense Technical Information Center Building 5, Cameron Station Alexandria, Virginia 22314	12	Mr. John Boyle Materials Branch Naval Ship Engineering Center Philadelphia, Pennsylvania 19112	1
DTNSRDC Attn: Dr. G. Bosmajian Applied Chemistry Division Annapolis, Maryland 21401	1	Naval Ocean Systems Center Attn: Dr. S. Yamamoto Marine Sciences Division San Diego, California 91232	1
Dr. William Tolles Superintendent Chemistry Division, Code 6100 Naval Research Laboratory Washington, D.C. 20375	1		

END

FILMED

1-85

DTIC